THE JOURNAL OF PHYSICAL CHEMISTRY B

Article

pubs.acs.org/JPCB

Behavior of Fluorescent Cholesterol Analogues Dehydroergosterol and Cholestatrienol in Lipid Bilayers: A Molecular Dynamics Study

João R. Robalo,[†,‡] António M. T. Martins do Canto,[†,‡] A. J. Palace Carvalho,[†,‡] J. P. Prates Ramalho,[†,‡] and Luís M. S. Loura*[,§,∥]

[†]Departamento de Química, Escola de Ciências e Tecnologia, and [‡]Centro de Química de Évora, Universidade de Évora, Rua Romão Ramalho, 59, 7000-671 Évora, Portugal

[§]Faculdade de Farmácia, Universidade de Coimbra, Pólo das Ciências da Saúde, Azinhaga de Santa Comba, 3000-548 Coimbra, Portugal

[∥]Centro de Química de Coimbra, Largo D. Dinis, Rua Larga, 3004-535 Coimbra, Portugal

Supporting Information

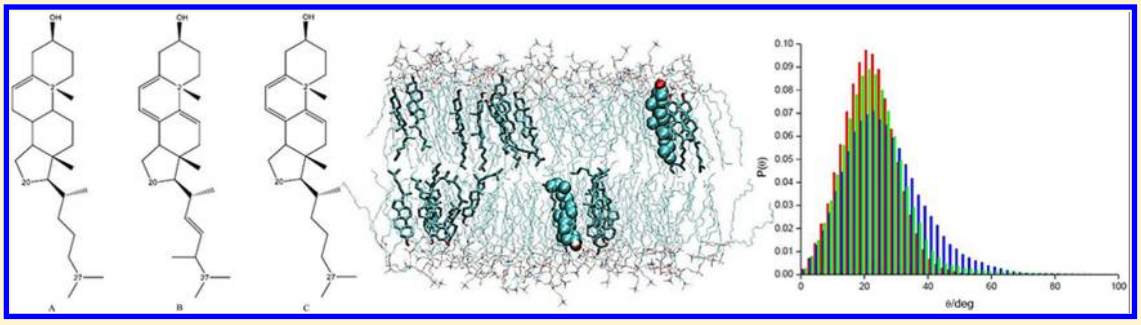

ABSTRACT: Molecular dynamics simulations of bilayer systems consisting of varying proportions of 1-palmitoyl-2-oleoyl-*sn*-glycero-3-phosphocholine (POPC), cholesterol (Chol), and intrinsically fluorescent Chol analogues dehydroergosterol (DHE) or cholestatrienol (CTL) were carried out to study in detail the extent to which these fluorescent probes mimic Chol's behavior (location, orientation, dynamics) in membranes as well as their effect on host bilayer structure and dynamics (namely their ability to induce membrane ordering in comparison with Chol). Control properties of POPC and POPC/Chol bilayers agree well with published experimental and simulation work. Both probes and Chol share similar structural and dynamical properties within the bilayers. Additionally, the fluorescent sterols induce membrane ordering to a similar (slightly lower) extent to that of Chol. These findings combined demonstrate that the two studied fluorescent sterols are adequate analogues of Chol, and may be used with advantage over side-chain labeled sterols. The small structural differences between the three studied sterols are responsible for the slight variations in the calculated properties, with CTL presenting a more similar behavior to Chol (correlating with its larger structural similarity to Chol) compared to DHE.

INTRODUCTION

Cholesterol (Chol; structure in Figure 1A) is a ubiquitous component of many biological membranes, including plasma membranes of mammals, in which it appears as the most abundant individual lipid species. Effects of Chol insertion include an increase in acyl chain order and bilayer thickening for fluid phospholipid membranes (and conversely for gel phase membranes), and physiological Chol concentrations can induce formation of a liquid ordered (lo) phase in phosphatidylcholine bilayers,[1−4] with properties intermediate between those of the fluid and the gel phases. Consequently, Chol plays an essential role in establishing proper membrane fluidity, permeability, and mechanical strength,[5−8] and its differential interaction with other membrane components (namely, phosphatidylcholine and sphingomyelin) is central to the formation of lipid rafts in cell membranes, which have been in turn implicated in signaling and trafficking processes.[9,10]

Several techniques may be used in the characterization of Chol's organization and dynamics in membranes, as well as its distribution in cells. Among them, fluorescence presents the advantage of allowing combination of spectroscopic and microscopic information. The former includes parameters that can be measured in steady-state (quantum yield, anisotropy) or time-resolved (intensity and anisotropy decays) conditions, and it allows monitoring of photophysical processes that are sensitive to distance, concentration (Förster Resonance Energy Transfer or FRET), aggregation (FRET, static quenching), or diffusion (collisional quenching). On the other hand, fluorescence imaging brings spatial resolution and the possibility of direct observation of Chol distribution and organization in both model (e.g., giant unilamellar vesicles) and cell membranes.[11] Although

Received: December 6, 2012
Revised: March 6, 2013
Published: April 18, 2013

   dx.doi.org/10.1021/jp312026u | *J. Phys. Chem. B* 2013, 117, 5806−5819

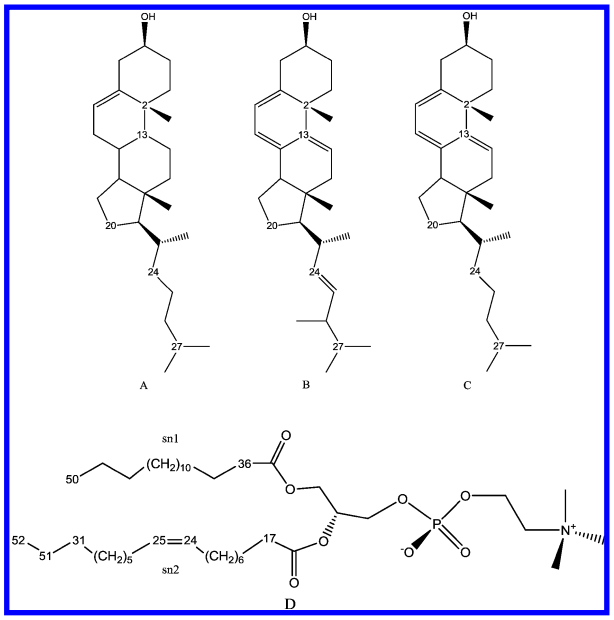

Figure 1. Structure of (A) Chol, (B) DHE, (C) CTL, and (D) POPC. Numbering of particular atoms mentioned in the text is also given.

Chol is not fluorescent and as such cannot be directly studied using fluorescence techniques, a large variety of fluorescent sterols, either bearing an extrinsic fluorescent label or exhibiting intrinsic fluorescence, are commercially available and have been widely used in membrane biophysics and cell biology.[12] Sterols with a fluorophore tag (either as cholesteryl esters or linked to the side chain) are often designed for convenient spectroscopic properties (e.g., high fluorescence quantum yield and molar absorption coefficient, emission environmental sensitivity, and/or photostability). However, their ability to mimic the behavior of Chol in membranes is highly questionable. For example, sterols labeled with the nitrobenzoxadiazole (NBD) moiety at the side chain show preference for the Chol-poor phase in a liquid ordered/liquid disordered lipid mixture[13] and may adopt an upside-down orientation within bilayers.[14] More promisingly, a sterol labeled at the side chain with the 4,4-difluoro-4-bora-3*a*,4*a*-diaza-*s*-indacene (BODIPY) fluorophore was found to partition into ordered domains in model membranes.[15] Molecular dynamics (MD) simulations of this BODIPY-Chol probe highlighted the similarity between the behaviors of this sterol and that of Chol in membranes, with slight differences in the effects upon area/lipid, membrane thickness, and deuterium order parameter ($-S_{CD}$).[16] However, this study also revealed the existence of two populations of fluorescent sterol differing in orientation: a predominant configuration, with an upright orientation of the steroid ring system (similar to Chol), and, for low sterol bilayers, a significant population with a more tilted steroid ring system, together with a slight upward loop of the BODIPY moiety.

An alternative approach is the use of fluorescent sterols with conjugated double bonds in the ring system, such as dehydroergosterol (DHE, Figure 1B) or cholestatrienol (CTL, Figure 1C). These molecules have structures close to that of Chol and have been shown to display similarities in behavior with this sterol. DHE is a naturally occurring sterol, synthesized by the yeast *Candida tropicalis* and the sponge *Biemna fortis*. Experimental evidence has suggested that DHE and Chol have qualitatively similar effects on host phospholipid bilayers (see Wüstner[12] and references therein). In particular, DHE is also able to induce ordered phases (although not as stiff as those induced by Chol), and partitions preferably to Chol-rich domains.[17] Whereas DHE's side chain differs from Chol by an additional methyl group and a double bond (rendering its structure closer to those of other sterols such as ergosterol and desmosterol), Chol and CTL share an identical side chain, which may enable closer mimicking of Chol's behavior by CTL when compared to DHE, as hinted from nuclear magnetic resonance measurements.[14] CTL, identically to DHE, possesses three conjugated double bonds in the ring system, responsible for its fluorescence emission (compared to the single double bond of Chol). 7-Dehydrocholesterol (7-DHC), which, with its two conjugated double bonds, has intermediate structure between those of Chol and CTL, forms lo phases with sphingomyelin, albeit in smaller and less clearly delineated domains as those observed in presence of Chol.[18] These studies are illustrative of a more general result, i.e., very small differences in sterol structure often result in sizable consequences for sterol properties in lipid membranes, with Chol's structure befitting its role as lead modulator of membrane properties.[19] In turn, these differences in membrane properties can have large biological significance. For example, the inability of 7-DHC to replace Chol as a component of cell membranes has been suggested as one of the probable causes of the cell defects associated to Smith-Lemli-Opitz syndrome (in which enzyme reduction of 7-dehydrocholesterol to Chol is blocked).[18] For these reasons, a detailed molecular-level comparison of the location, orientation, dynamics, and effects on bilayer properties of fluorescent sterols, and Chol is important to fully understand the extent to which these probes are good Chol analogues.

To this effect, MD simulation is a useful method for the characterization of lipid membrane systems (see, e.g., the recent review by Lyubartsev and Rabinovich,[20] and references therein) and, in particular, to realize the behavior of fluorescent probes upon incorporation in lipid bilayers.[21,22] Because MD simulations enable simultaneous and independent monitoring of the probe and lipid molecules, they can be used to characterize the location and dynamics of membrane probes, as well as the extent of perturbation they induce on the host lipid structure. MD has been previously used to compare the behavior of Chol to that of other structurally related sterols, such as ergosterol, lanosterol,[23] desmosterol, demethylated cholesterol,[24] 7-DHC, and ketosterol.[25−28] However, to our knowledge, the sole previously published MD study of lipid bilayers containing fluorescent Chol analogues is that of BODIPY-Chol mentioned above. This work employs MD simulation to study the behavior of DHE and CTL in lipid bilayers of 1-palmitoyl-2-oleoyl-*sn*-glycero-3-phosphocholine (POPC) containing variable amounts of sterol (2 sterol molecules in a 128-phospholipid bilayer, 20 mol % and 50 mol % sterol). The ability of DHE and CTL to mimic Chol in the different systems is evaluated by assessment of both sterol (location, orientation, dynamics) and phospholipid (area/lipid, bilayer thickness, acyl chain tilt, and order parameters, dynamics) properties.

SIMULATION DETAILS

The topology of the POPC molecule (using a united-atom description for CH, CH_2, and CH_3 groups, based on the parameters presented by Berger et al.[29] for 1,2-dipalmitoyl-*sn*-glycero-3-phosphatidylcholine (DPPC)) and the coordinate file of a POPC bilayer were obtained from Dr. Peter Tieleman's group webpage (http://moose.bio.ucalgary.ca/index.php?page=Structures_and_Topologies).[30] The SPC water model was used.[31] Chol model molecules and their bonded and nonbonded

dx.doi.org/10.1021/jp312026u | J. Phys. Chem. B 2013, 117, 5806−5819

parameters were taken from Höltje et al.[32] and were downloaded from the GROMACS web page (http://www.gromacs.org/index.php?title=Download_%26_Installation/User_contributions/Molecule_topologies). Probes' structures were obtained through geometry optimization at the R-DFT/B3LYP/6-31G*[33−36] level of theory under the Firefly QC package,[37] and topologies were created by submission of the optimized geometry to the PRODRG topology server.[38] The resulting polar hydrogen-only united atoms topology was adjusted by adopting the partial charges from the Chol topology, given the likeness of Chol and probe structural and electronic properties. Figure 1 presents the structures of the four bilayer molecules considered in this study.

Four bilayer models, with varying Chol content, were initially assembled using the VMD software.[39] All bilayers were hydrated with excess water,[40] to a solvent/lipid ratio higher than 30. The numbers of lipid molecules in each system were 128 POPC (0 mol % Chol), 126 POPC:2 Chol (~1.6 mol % Chol, for the purpose of comparing the behavior of Chol and Chol analogues in a liquid disordered bilayer), 96 POPC:24 Chol (20 mol % Chol), and 72 POPC:72 Chol (50 mol % Chol). Six bilayers containing two Chol analogue molecules (either DHE or CTL, one molecule in each leaflet) were obtained by addition or replacement of two Chol molecules, thus producing 126 POPC:2 DHE, 126 POPC:2 CTL, 96 POPC:22 Chol:2 DHE, 96 POPC:22 Chol: 2 CTL, 72 POPC:72 Chol:2 DHE, and 72 POPC:72 Chol:2 CTL systems. These simulations were carried out to study both DHE and CTL's behavior as Chol's fluorescent analogues. Second, both 20 mol % Chol and 50 mol % Chol bilayers were modified by replacing all Chol molecules with either DHE or CTL. This unphysical (given the use of these molecules as fluorescent reporters, generally not exceeding ~2−5 mol % in the membrane) complete replacement of Chol by each probe aimed at a more clear assessment of the probe effects on the structural and dynamics of the bilayers, compared to Chol, as well as a better statistical evaluation of probe properties in ordered bilayers, and comparison with an experimental NMR study,[14] wherein some of the measured samples possess large amounts of DHE or CTL. This led to the 96 POPC:24 DHE, 96 POPC:24 CTL, 72 POPC:72 DHE, and 72 POPC:72 CTL systems. Table 1 summarizes the number of molecules of each species involved in the 14 simulated systems.

Starting configurations were subject to an energy minimization run using the steepest descent algorithm, after which a short run (10 ps, 1 fs time step, and all remaining parameters as described for the production run) was carried out. Finally, a production simulation was run for 100 ns (4 fs time step) under the NPT ensemble and periodic boundary conditions, using Berendsen coupling schemes for both pressure (semi-isotropic; 1 bar; 1.0 ps coupling time) and temperature (300 K; 0.1 ps coupling time).[41] The use of such a time step was made possible by constraining bond lengths and angles to their equilibrium values, using the SETTLE algorithm[42] for water and the LINCS algorithm[43] for all other bonds (see also discussion in Feenstra et al.[44] and Anézo et al.[45]). van der Waals and Coulomb interactions were cut off at 1.0 nm, whereas for long-range electrostatics, the Particle Mesh Ewald (fourth-order interpolation along with 0.12 nm grid spacing for FFT) treatment[46] was applied. All simulations and analyses were carried out using the *GROMACS* 3.3 software package.[47−50] For analysis, the final 25 ns of each production run were used, unless stated otherwise.

Table 1. Composition of the Systems Studied in the Present Work[a]

system	n_{POPC}	n_{Chol}	n_{DHE}	n_{CTL}
A	128	—	—	—
B	126	2	—	—
C	126	—	2	—
D	126	—	—	2
E	96	24	—	—
F	96	22	2	—
G	96	22	—	2
H	96	—	24	—
I	96	—	—	24
J	72	72	—	—
K	72	72	2	—
L	72	72	—	2
M	72	—	72	—
N	72	—	—	72

[a] n_i denotes the number of molecules of species i in each simulated system (abbreviations are as used in the text).

RESULTS AND DISCUSSION

Figure S1 in the Supporting Information file depicts the final structures obtained in each of the simulated systems. It is clear from simple visual inspection of the figure that (i) increasing the sterol content leads to increased ordering of the bilayer, judging from the apparent higher fraction of *trans* conformations in POPC acyl chains (this occurs not only with Chol, as widely known, but also with the fluorescent sterol probes); (ii) the main features of location and orientation of DHE and CTL in the bilayers are the same as those of Chol (hydroxyl group located near the glycerol/carbonyl moieties of POPC, molecule mostly oriented perpendicularly to the bilayer plane). These findings will be discussed at length in the following sections, where similarities and differences between the properties/effects of the three sterols will be quantitatively assessed.

The time variation of the area per lipid is a common indicator of the equilibration of the bilayer, whereas its average value is often used to assess the adequacy of the simulation methodology, due to its sensitiveness to simulation details.[45] For this purpose, Figure S2 in the Supporting Information file shows that the initial configurations rapidly approach equilibrium. In this figure, individual molecular areas of each component are shown. These are described and discussed in more detail below, regarding the effect of the different sterols on the bilayer. For the moment, we start by focusing on the properties of the sterol probes (location, orientation, and dynamics), in comparison with Chol, before switching to the bilayer lipids' structural and dynamical properties.

Sterol Probes' Location and Orientation. Figure 2A shows the average transverse locations of the sterols' O atoms, ring system center of mass, and side-chain C27 atoms, all relative to the bilayer midplane. It is clear that, as the membrane is loaded with sterol, the distances between each atom and the center of the bilayer increase. Curiously, this effect is not so pronounced for the side-chain C27 as for the O atoms and the ring system center of mass, which is a first indication that, as the bilayers are enriched with sterol, the latter molecules adopt a more upright conformation (see also below, the analysis of sterol axis tilt). On the other hand, distances of the selected sterol locations to POPC's P atom (shown in Figure 2B) remain almost invariant. In combination, these results indicate that, as the bilayers become thicker for higher sterol concentrations (see below), sterol

dx.doi.org/10.1021/jp312026u | J. Phys. Chem. B 2013, 117, 5806−5819

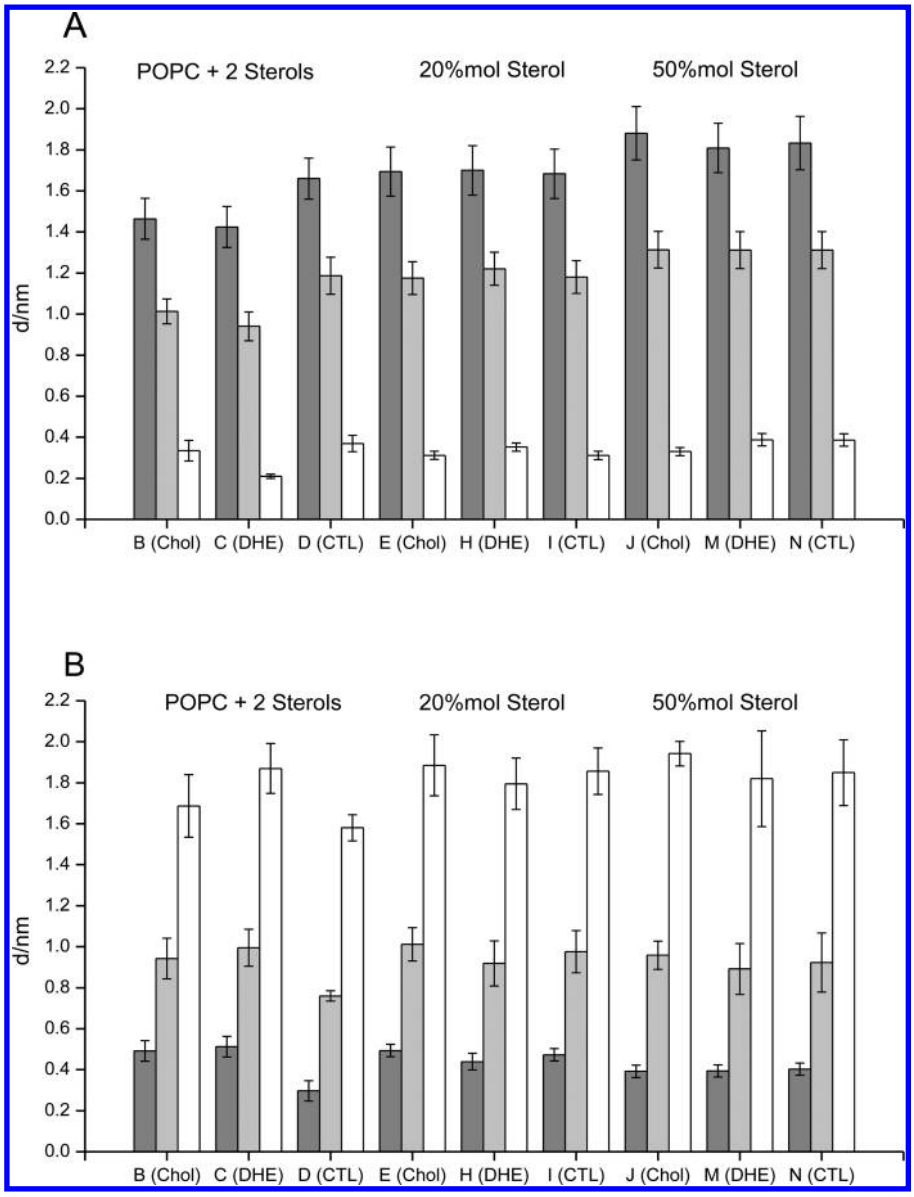

Figure 2. Average distance (d) between (A) bilayer center and sterol's O atom (dark gray), center of mass of the four sterol rings (gray), and sterol C27 atom (white) and (B) POPC P atom and Sterol's O atom (dark gray), center of mass of the four rings (gray) and C27 atom (white).

location relative to the POPC headgroups is unchanged, while distance to the bilayer center increases. Clearly, with the exception of systems B, C, and D, for which the limited averaging over only two sterol molecules affects the calculation accuracy, the average location of the different atoms is similar for the three studied sterols. On close inspection, it can be seen that for 50 mol % sterol, Chol O is located at a slightly (nonsignificantly) larger distance to the center than DHE O and CTL O atoms. However, this is probably the result of an increased bilayer thickening induced by Chol in comparison with the other sterols (see below), and it can be concluded that all sterols have similar relative depths when embedded in membranes with corresponding composition. This behavior has been observed in MD comparative studies of other structurally related sterols, including demethylated cholesterol,[24] desmosterol, and 7-DHC.[28]

This similarity is reinforced by inspection of the mass density profiles of the different system components across the bilayers (Figure 3), which display no significant differences for equal amounts of total sterol. The sole off-trend result is the somewhat awkward profile of DHE in panel B. This probably reflects poor statistics resulting from its calculation using only two sterol molecules, which probably also caused the lower values of distance of sterol atom groups to the bilayers center in Figure 2A (system C).

Tilts of the sterol long axis (defined as the vector uniting atoms 2 and 20 of each sterol; see Figure 1) relative to the bilayer normal were calculated. The corresponding distributions are shown in Figure 4 for 20 and 50 mol % of sterol (only DHE and CTL simulations with complete replacement of Chol are shown, as the ones with only two replaced molecules gave similar, albeit more variable results). It can be seen that all orientation distributions are similar in shape, with average values located around 30−40° for 20 mol % sterol ((31 ± 2)° for Chol, (31 ± 1)° for CTL, and (39 ± 1)° for DHE) and 20−25° for 50 mol % ((22.1 ± 0.4)° for Chol, (22.3 ± 0.4)° for CTL, and (25.0 ± 0.2)° for DHE). The value for 20 mol % Chol agrees with that obtained for POPC/Chol (33°; 22 mol % sterol) by Róg and

dx.doi.org/10.1021/jp312026u | J. Phys. Chem. B 2013, 117, 5806−5819

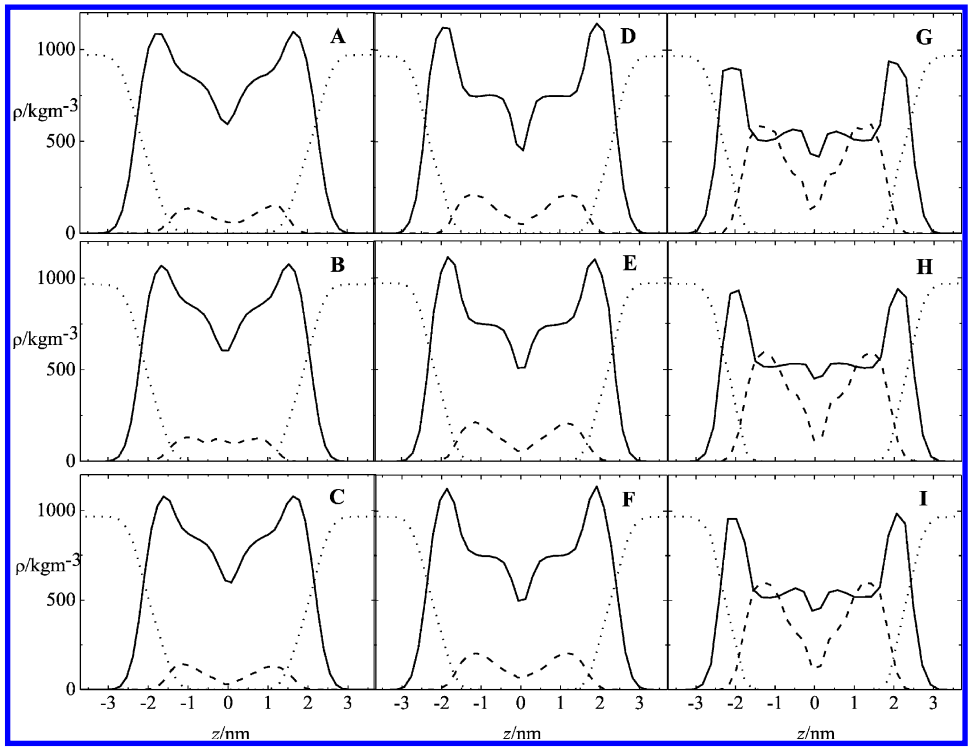

Figure 3. Mass density profiles for systems with 2 sterol molecules (A: Chol; B: DHE; C: CTL), 20 mol % sterol (D: Chol; E: DHE; F: CTL), and 50 mol % sterol (G: Chol; H: DHE; I: CTL). In all plots, solid, dotted, and dashed lines represent profiles of POPC, water, and sterol, respectively. Sterol profiles were multiplied by a factor of 10 in plots A–C for better visualization.

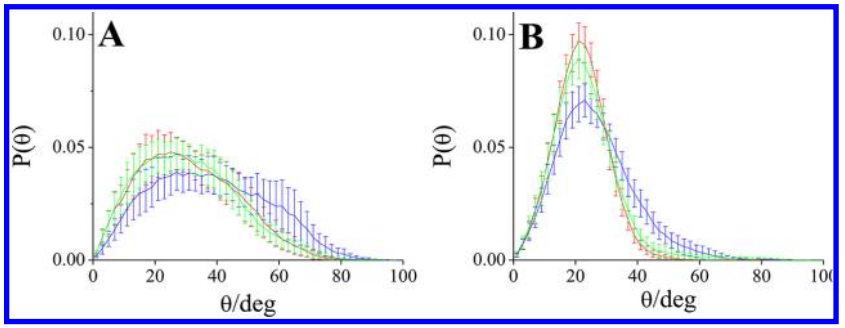

Figure 4. Probability density functions $P(\theta)$ of the angle between the sterol long axis and the bilayer normal for 20 mol % (A) and 50 mol % (B) sterol; in all plots, red, blue, and green lines refer to Chol, DHE, and CTL, respectively.

Pasenkiewicz-Gierula.[51] The shift to lower values observed upon increasing sterol content is again rationalized taking into account sterol-induced membrane ordering. For each sterol fraction, it can be seen that, whereas Chol and CTL have almost identical orientation distributions, that of DHE appears significantly displaced to larger tilt values (especially for 20 mol % sterol). This is a first indication that, of the two fluorescent sterols, CTL is the one with the behavior most similar to that of Chol. In any case, orientations of all sterols are similar overall, in agreement with the ^{1}H magic angle spinning nuclear Overhauser enhancement spectroscopy data of Scheidt et al.[14] Taking into account the reported inverse correlation between sterol tilt and ordering ability,[27] the increased tilt of DHE also anticipates a less efficient ordering of the bilayer (see below).

Radial distribution functions (RDFs) of both POPC (panels A, C) and Chol (panels B, D) centers of mass around the different sterols are shown in Figure 5, for the systems with 20 mol % (systems E, F, G; panels A, B) and 50 mol % Chol (systems J, K, L; panels C, D). Whereas RDFs of POPC around the sterols are very similar, there are some noticeable differences in the RDFs of Chol. For 20 mol % Chol, the RDF of Chol around DHE is generally lower than those around Chol and CTL. This is probably related to the above-mentioned differences in DHE and Chol tilt, which will affect packing and distribution of Chol around DHE. This effect is no longer clear for 50 mol % Chol, probably because, for these highly ordered systems, tilt differences are not so evident (see Figure 4B). On the other hand, unlike those around DHE, the RDFs of Chol around CTL are very similar for both compositions to those around Chol, in agreement with the similarity between Chol and CTL's orientations.

Another way to characterize lipid packing around the sterols is to calculate the number of POPC neighboring atoms for different positions in the sterol molecule. This is shown in Figure 6 for the three sterols in systems B, C, and D. Differences between the three sterols are not significant for O6 and C13 sterol atoms, which are located at the hydrophilic end of the molecule and near the center of the steroid ring system, respectively. However, lipid

dx.doi.org/10.1021/jp312026u | J. Phys. Chem. B 2013, 117, 5806–5819

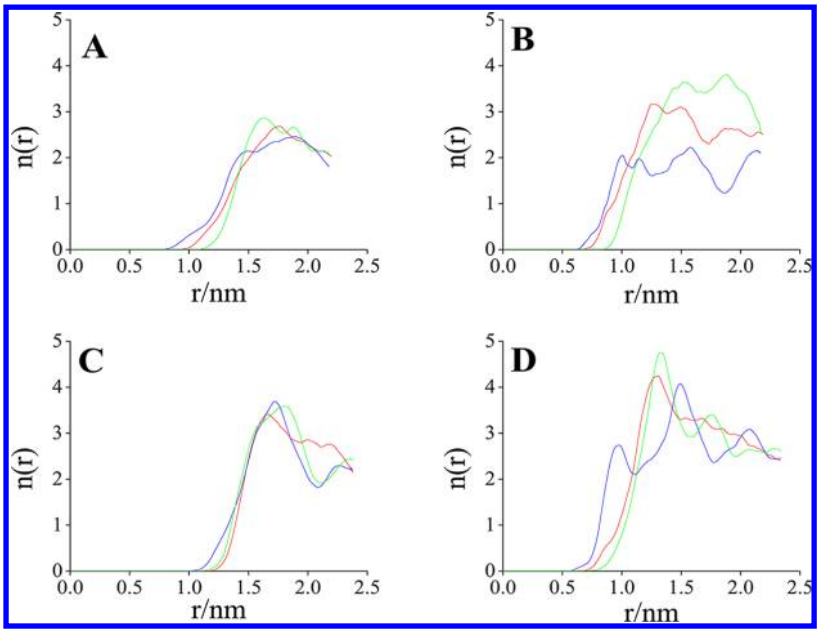

Figure 5. Radial distribution function of POPC (A,C) and Chol (B,D) center of mass around Chol (red), DHE (blue), or CTL (green) center of mass in 20% Chol (A,B; systems E, F, and G) and 50% Chol (C,D; systems J, K, and L) bilayers.

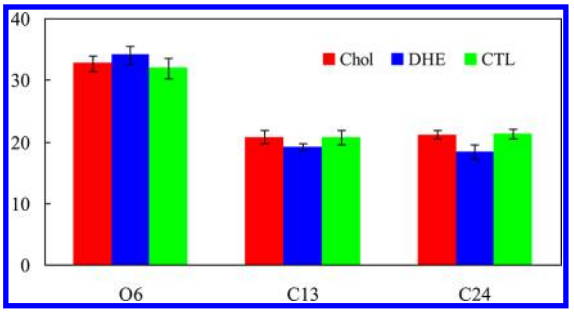

Figure 6. Average number of neighboring (distance <0.6 nm) POPC atoms around selected sterol atoms in systems B (Chol), C (DHE), and D (CTL).

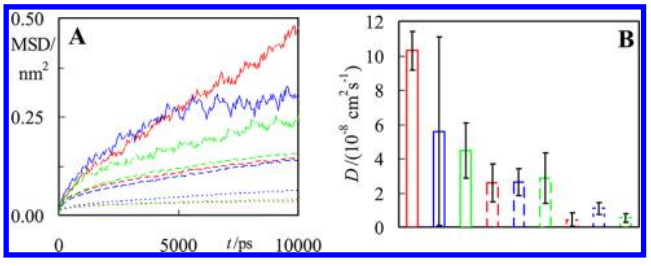

Figure 7. Lateral diffusion of sterols in POPC and POPC/Chol bilayers: mean square displacements (MSD; A) and diffusion coefficients (B). Red, blue, and green lines refer to Chol, DHE, and CTL, respectively. Solid, dashed, and dotted lines refer to POPC (with two sterol molecules), POPC/20 mol % sterol, and POPC/50 mol % sterol systems, respectively.

packing around DHE C24 atom (one of the atoms involved in this sterol's tail double bond; see Figure 1) is significantly less tight than around the corresponding atoms of Chol and CTL. These observations can be related to the comparative study of Chol, 7-DHC, and desmosterol by Róg et al.[28] In agreement with our results, relatively minor effects were observed in the ring atoms' neighbors upon replacing Chol by 7-DHC (which has an additional bond in the ring system compared to Chol, and one less than both DHE and CTL). Additionally, in these authors' study, the number of neighbors around desmosterol and Chol tail atoms, including C24, was calculated in both DPPC and DOPC bilayers. Similarly to DHE, desmosterol has a double bond in the side-chain, although it lacks the additional tail methyl group of DHE (as well as the two additional steroid ring double bonds). Very minor differences were observed by these authors between desmosterol and Chol in unsaturated DOPC bilayers, while a larger difference was apparent in saturated DPPC membranes. The fact that, in our study, significant differences were observed between DHE and Chol (and CTL) may be attributed to the intermediate nature of POPC compared to DPPC and DOPC (with one saturated and one unsaturated acyl chains), combined with the more extensive structural differences between DHE's tail and those of the other sterols.

Probe Dynamical Properties. Lateral diffusion of Chol in the binary POPC/Chol systems (B, E, J) was compared to that of the sterol probes in the corresponding systems with two inserted fluorescence probe molecules (C, F, and K for DHE; D, G, and L for CTL). To this effect, lateral diffusion coefficients D were calculated from the two-dimensional mean square displacement (MSD), using the Einstein relation

$$D = \frac{1}{4} \lim_{t\to\infty} \frac{\mathrm{dMSD}(t)}{\mathrm{d}t} \tag{1}$$

In turn, MSD is defined by

$$\mathrm{MSD}(t) = \langle \| \vec{r}_i(t + t_0) - \vec{r}_i(t_0) \|^2 \rangle \tag{2}$$

where $\vec{r}_i$ is the (x, y) position of the center of mass of molecule i of a given species; the averaging is carried out over all molecules of this kind and time origins t_0. To eliminate noise due to fluctuations in the center of mass of each monolayer, all MSD analyses were carried out using trajectories with fixed center of mass of one of the monolayers, and the final result is averaged over the two leaflets.

Figure 7A shows MSD(t) for the above-mentioned systems, whereas the corresponding D values are presented in Figure 7B. Because of the small number of probe molecules (two), there is a

dx.doi.org/10.1021/jp312026u | J. Phys. Chem. B 2013, 117, 5806−5819

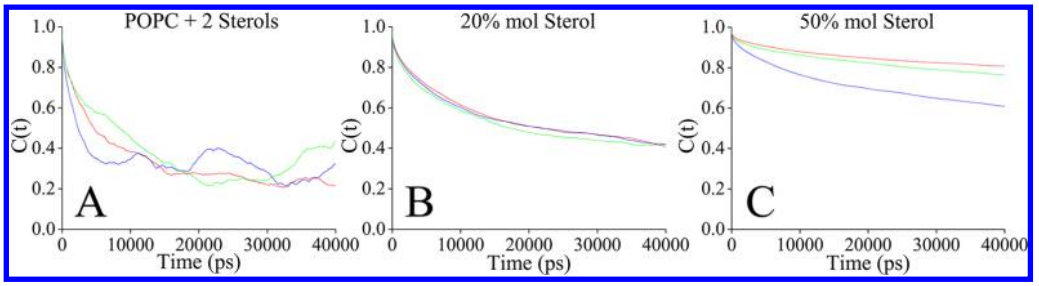

Figure 8. Rotational autocorrelation functions $C(t)$ for the sterol long axis in binary POPC/sterol mixtures with ~1.5 mol % (A), 20 mol % (B), or 50 mol % (C) sterol. In all plots, red, blue, and green lines refer to Chol, DHE, and CTL, respectively.

Table 2. Average Values of Molecular Volume of POPC, Molecular Areas of All Bilayer Components, and Membrane Thickness for All Studied Systems

System	v_{POPC}/nm^3	a_{POPC}/nm^2	a_{Chol}/nm^2	a_{DHE}/nm^2	a_{CTL}/nm^2	Membrane thickness/nm
A	1.292 ± 0.040	0.636 ± 0.020	—	—	—	3.880 ± 0.276
B	1.289 ± 0.041	0.632 ± 0.022	0.291 ± 0.010	—	—	3.911 ± 0.268
C	1.287 ± 0.041	0.638 ± 0.020	—	0.303 ± 0.010	-	3.871 ± 0.271
D	1.286 ± 0.040	0.635 ± 0.019	—	—	0.287 ± 0.009	3.846 ± 0.276
E	1.264 ± 0.040	0.553 ± 0.019	0.261 ± 0.010	—	—	4.375 ± 0.302
F	1.267 ± 0.040	0.563 ± 0.020	0.263 ± 0.009	0.272 ± 0.009	-	4.313 ± 0.303
G	1.267 ± 0.040	0.556 ± 0.021	0.260 ± 0.010	—	0.255 ± 0.009	4.362 ± 0.297
H	1.270 ± 0.040	0.568 ± 0.019	—	0.273 ± 0.009	—	4.279 ± 0.303
I	1.268 ± 0.040	0.562 ± 0.020	—	—	0.258 ± 0.009	4.312 ± 0.297
J	1.262 ± 0.040	0.537 ± 0.020	0.252 ± 0.009	—	—	4.545 ± 0.315
K	1.262 ± 0.040	0.541 ± 0.019	0.254 ± 0.009	0.262 ± 0.009	—	4.503 ± 0.310
L	1.260 ± 0.040	0.539 ± 0.019	0.253 ± 0.009	—	0.249 ± 0.009	4.501 ± 0.312
M	1.255 ± 0.041	0.555 ± 0.021	—	0.271 ± 0.010	—	4.406 ± 0.301
N	1.248 ± 0.040	0.542 ± 0.021	—	—	0.252 ± 0.010	4.471 ± 0.309

large uncertainty associated with the calculated D values. Nevertheless, it is found that the diffusion coefficients of the three sterols are of the same order of magnitude for systems with identical Chol content. The sole exception is the CTL diffusion coefficient in POPC, which appears to be significantly smaller than that of Chol. Additionally, it is verified that increasing the Chol content in the bilayer leads to clear slowing of lateral diffusion, as expected.

In order to study the rotational dynamics of the probes in comparison with that of Chol, a rotational autocorrelation function $C(t)$ of the cholesterol long axis (C2−C20) was calculated, as defined below:

$$C(t) = \langle P_2(\cos\theta(\xi))\rangle \tag{3}$$

where $\theta(\xi)$, for the sake of commodity, is the angle between a vector defined in the molecular framework at times ξ and $t + \xi$, and $P_2(x) = (3x^2 - 1)/2$ is the second Legendre polynomial. Averaging is performed over ξ, which assuming a sufficiently ergodic trajectory is an approximation of the ensemble average.

Figure 8 shows the $C(t)$ curves obtained for the three sterols for different sterol content. For all systems, small but finite residual values of $C(t)$ are observed at long times, that is, these functions appear to have finite limits as $t \to \infty$. This is expected for probes embedded in lipid bilayers, and may arise from "wobbling-in-cone"-type hindered rotation.[52] The plots for the POPC + 2 sterol molecules' systems (panel A) are affected by poor statistics, as only two molecules were used in averaging. In any case, it is clear that for this composition the limiting values are low for the three species, indicating a relatively unhindered rotation. Upon increasing sterol content to 20 mol % (panel B) and 50 mol % (panel C), sterol rotation becomes slower, and the extent of decrease of $C(t)$ during the studied time window is clearly smaller. Differences between the sterols are not significant up to 20 mol % sterol, indicating that intrinsically the three species have very similar rotational mobilities in these systems. However, for 50 mol % sterol, the decreased sterol-induced ordering of the bilayer by DHE (see below) leads to clearly faster rotational tumbling in comparison with Chol and CTL. This is not apparent in systems F and G, where only 2 Chol molecules were replaced by DHE or CTL (respectively; not shown). Therefore, it seems that differences apparent in Figure 8C stem mostly from the overall physical properties of the particular bilayers (more ordered for Chol (system L) and CTL (system N) than DHE (system M), see also below), and the three sterols behave as almost identical rotors, as expected from their very similar structures.

Molecular Areas and Bilayer Thickness. The instant area per lipid molecule, a, was calculated for the pure POPC bilayer as the instant box area divided by the number of lipid molecules in each leaflet (64). For the mixed bilayer systems, the procedure of Hofsäß et al.[53] was used. In summary, the molecular area of POPC was obtained as

$$a_{POPC} = 2v_{POPC}/h \tag{4}$$

where

$$v_{POPC} = \frac{V - n_w v_w - n_{Chol} v_{Chol} - n_{Probe} v_{Probe}}{n_{POPC}} \tag{5}$$

is the molecular volume of POPC, and

$$h = \frac{V - n_w v_w}{A} \tag{6}$$

dx.doi.org/10.1021/jp312026u | J. Phys. Chem. B 2013, 117, 5806−5819

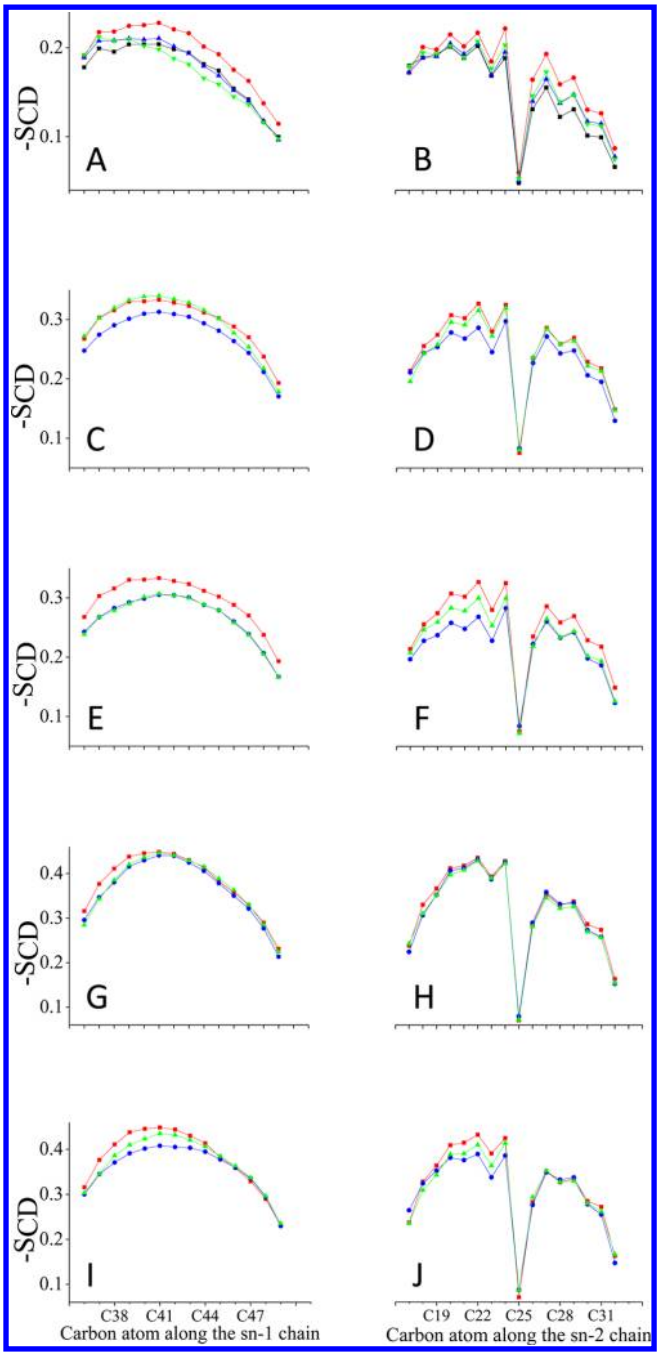

Figure 9. Deuterium order parameters ($-S_{CD}$) of POPC *sn*-1 (A, C, E, G, I) and *sn*-2 (B, D, F, H, J) for pure POPC and POPC + 2 sterol bilayers (A, B), 20 mol % total sterol (C–F), and 50 mol % total sterol (G–J). Panels C, D, G, and H concern systems where two Chol molecules were replaced with probes, whereas panels E, F, I, and J show the profiles obtained upon complete replacement of Chol by fluorescent sterol. In all plots, black, red, blue, and green refer to POPC, Chol, DHE, and CTL, respectively.

In turn, V and A are the instant simulation box volume and area, respectively, whereas n_i and v_i denote number of molecules and molecular volume of species i ($i = w$ indicates water). For two-component (POPC/sterol) bilayers, the sterol molecular area was computed by

$$a_{\text{Sterol}} = \frac{2A - n_{\text{POPC}}a_{\text{POPC}}}{n_{\text{Sterol}}} \quad (7)$$

whereas for ternary (POPC/Chol/probe sterol) systems, the following two equations were used for calculation of the sterols' molecular areas:

$$a_{\text{Chol}} = \frac{2Av_{\text{Chol}}}{V - n_w v_w} \quad (8)$$

$$a_{\text{Probe}} = \frac{2A - n_{\text{POPC}}a_{\text{POPC}} - n_{\text{Chol}}a_{\text{Chol}}}{n_{\text{Probe}}} \quad (9)$$

In these calculations, it was assumed that $v_W = 0.03$ nm^3 and Chol had a fixed molecular volume (based on crystallography data[53]) of $v_{\text{Chol}} = 0.593$ nm^3. Molecular volumes of both probe sterols, also used in all systems involving these species, were obtained using the 3 V volume calculator of Voss et al.,[54] yielding $v_{\text{DHE}} = 0.612$ nm^3 and $v_{\text{CTL}} = 0.582$ nm^3. These values are consistent with that of v_{Chol}, as CTL has four H atoms less than Chol, whereas DHE, while also having four H atoms less, has an additional C atom. On the other hand, v_{POPC} was calculated for each system using eq 5, and its average values are shown in Table 2, together with those of the molecular areas of each component, which time traces are also depicted in Figure S2. Bilayer thickness was calculated as the distance between the average transverse locations of the P atoms in opposing leaflets, and its average values are also shown in the table.

The molecular volume of POPC agrees well (within the calculated uncertainty, taking into account its estimation from difference between the simulation box volume, and the volumes taken up by water and sterol) with the 1.2565 nm^3 experimental value of Greenwood et al.[55] On the other hand, the results of area per lipid for pure POPC (system A) agree with the experimental values of 0.65 nm^2 ($T = 298$ K),[56] 0.64 nm^2 ($T = 298$ K),[57] and 0.63 nm^2 ($T = 297$ K),[58] as well as with those obtained from MD simulations by Böckmann et al.[59] ($T = 300$ K, $a = 0.655$ nm^2), Mukhopadhyay et al.[60] ($T = 298$ K, $a = 0.62$ nm^2), Gurtovenko and Anwar[61] ($T = 310$ K, $a = 0.65$ nm^2), and Pandit et al.[62] ($T = 303$ K, $a = 0.630$ nm^2). The results for the POPC/Chol systems (B, E, J) show the well-known trend for diminishing volume and area per lipid as well as increasing bilayer thickness as the Chol concentration increases (Chol condensing and ordering effect; see Hung et al.,[63] Róg et al.,[64] and references cited therein). Also, Pandit et al.[62] reported POPC areas of 0.567 nm^2 for 10 mol % Chol and 0.445 nm^2 for 30% Chol, respectively, above and below our 4:1 POPC:Chol's a_{POPC} value. It is apparent that sterol probes mimic this behavior qualitatively, as a_{POPC} decreases monotonically for binary bilayers with increasing amounts of DHE (systems C, H, M) or CTL (systems D, I, N). However, condensation by the fluorescent sterols in these systems is probably not as efficient as that produced by Chol. In fact, for identical sterol concentration, the systems containing Chol (B, E, J) are consistently the ones for which the calculated a_{POPC} is lower (although the differences are generally smaller than the estimated uncertainty). This is clear in the POPC + 2 sterols systems, where a_{POPC} and bilayer thickness show ~2% variations upon replacement of Chol (system B) with fluorescent sterols (systems C, D), rendering these parameters' values identical to those calculated for pure POPC (system A). In contrast, Chol already appears to induce a small degree of ordering even at this low concentration. This set of simulations also already illustrates that, whereas the calculated molecular areas of Chol and CTL are similar, that of DHE is slightly larger.

For higher amounts of total sterol (20 mol %, systems E–I; 50 mol %, systems J–N), condensation is consistently maximal

dx.doi.org/10.1021/jp312026u | J. Phys. Chem. B 2013, 117, 5806–5819

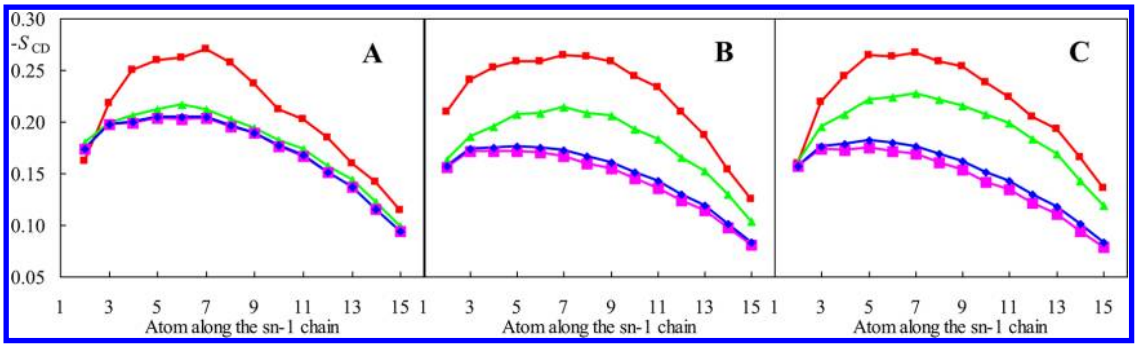

Figure 10. Deuterium order parameters ($-S_{CD}$) of POPC *sn*-1 chain for different ranges of distance R to the closest sterol molecule: R < 0.6 nm (red), 0.6 nm < R < 1.2 nm (green), and R > 1.2 nm (magenta). The blue curve is the average $-S_{CD}$ profiles taking into account all configurations. All panels refer to 126 POPC: 2 Sterol systems (panel A, Chol; panel B, DHE; panel C, CTL).

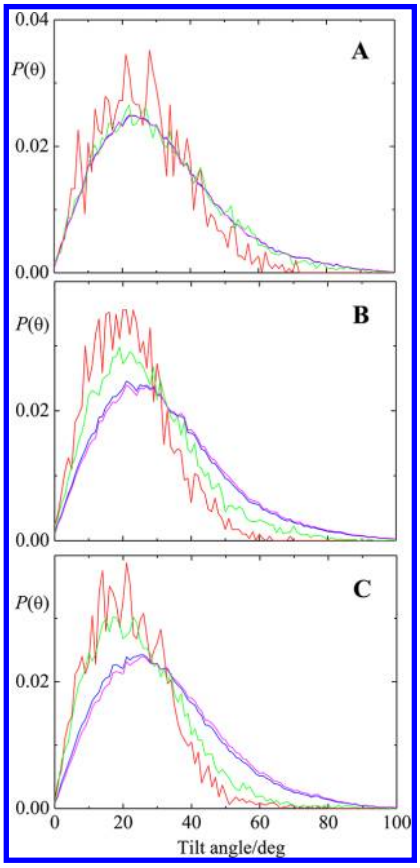

Figure 11. Tilt of of POPC *sn*-1 chains for different ranges of distance R to the closest sterol molecule: R < 0.6 nm (red), 0.6 nm < R < 1.2 nm (green), and R > 1.2 nm (magenta). The blue curve are the average tilt distributions taking into account all configurations. All panels refer to 126 POPC:2 Sterol systems (panel A, Chol; panel B, DHE; panel C, CTL).

(lowest a_{POPC}) for the POPC/Chol binary bilayer (E for 20 mol %, J for 50 mol %). Replacement of two Chol molecules by DHE (F for 20 mol %, K for 50 mol %) or CTL (G for 20 mol %, L for 50 mol %) already results in slight (smaller than the estimated uncertainty) but consistent effects (increase in a_{POPC}, and general decrease in bilayer thickness). However, as the total sterol concentration increases, the effect of replacing 2 Chol molecules with fluorescent probe becomes less important, and is almost unnoticeable for 50 mol % sterol. The high degree of organization imposed by Chol supersedes the smaller effect caused by DHE or CTL, which is well understood by noting that the relative degree of Chol replacement progressively decreases from the POPC + 2 sterols systems (100%) to those with 20 mol % sterol set (8%) and those with 50 mol % sterol set (3%). However, remarkable effects are still apparent upon replacing all Chol molecules with DHE (systems H for 20 mol %, or M for 50 mol %) or CTL (systems I for 20 mol %, or N for 50 mol %), emphasizing that these sterols do not produce as large a condensation effect as that of Chol. By comparing DHE with CTL, it is clear that DHE is the sterol presenting the smaller condensation effect, and the effects of CTL generally fall in between those of Chol and DHE. Variations of bilayer thickness generally follow the opposite trend observed for a_{POPC}, as expected.

Regarding the sterol molecular areas, they are rather similar, and, in close inspection, mostly increase in the order a_{CTL} < a_{Chol} < a_{DHE}, regardless of sterol concentration. The slightly lower molecular area of CTL relative to Chol (apparent for 20 mol % and 50 mol % sterol) may be due to the more restricted geometry imposed by the existence of three conjugated bonds in its ring system. On the other hand, DHE's molecular area is the largest of the three sterols for all sets of simulations, probably on account of the additional methyl group in the side chain (Figure 1), which implies a rougher contact surface with other bilayer constituents. This larger cross-sectional area of DHE is also consistent with the higher average tilt of this sterol compared with Chol and CTL (Figure 4). As expected from the increased bilayer order as the sterol content rises, all individual sterol molecular areas decrease from the 126 POPC:2 sterol to the 50 mol % sterol systems. Molecular volumes of POPC generally decrease with sterol content. Differences between fluorescently labeled and unlabeled systems of equal total sterol content become insignificant for 50 mol % sterol, reflecting the effect discussed above of smaller relative degree of replacement.

Probe Effects on POPC Chain Order Parameters and Chol Tilt Angles. In our simulations, using a united atom force field, deuterium order parameters (S_{CD}) for saturated (S_{CD}^{sat}) and unsaturated (S_{CD}^{unsat}) carbons are determined using the following relations:[65]

$$-S_{CD}^{sat} = \frac{2}{3}S_{xx} + \frac{1}{3}S_{yy} \quad (10)$$

$$-S_{CD}^{unsat} = \frac{1}{4}S_{zz} + \frac{3}{4}S_{yy} + \frac{\sqrt{3}}{2}S_{xy} \quad (11)$$

where S_{ab} are the order tensor coordinates, given by

dx.doi.org/10.1021/jp312026u | J. Phys. Chem. B 2013, 117, 5806−5819

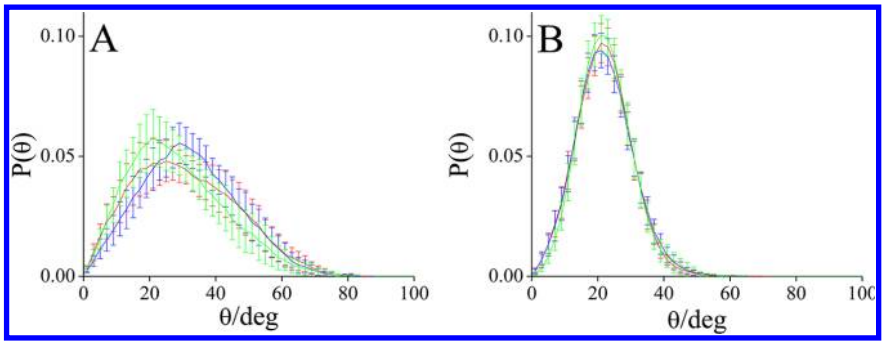

Figure 12. Probability density functions $P(\theta)$ of the angle between Chol long axis and the bilayer normal, in the absence (systems E and J) or presence of probe sterols (systems F, G, K, and L), for 20 mol % (A) and 50 mol % (B) total sterol. In all plots, red, blue, and green refer to Chol, DHE, and CTL, respectively.

Table 3. Lateral Diffusion Coefficients (D_{lat}) of POPC for Varying Sterol Nature and Content

system	D_{lat}(POPC)/10^{-8} cm^2 s^{-1}	system	D_{lat}(POPC)/10^{-8} cm^2 s^{-1}
A (no sterol)	6.7 ± 0.2	H (20 mol % DHE)	2.1 ± 0.3
B (1.5 mol % Chol)	4.4 ± 0.4	I (20 mol % CTL)	2.2 ± 0.3
C (1.5 mol % DHE)	6.4 ± 1.2	J (50 mol % Chol)	0.48 ± 0.02
D (1.5 mol % CTL)	5.6 ± 0.7	M (50 mol % DHE)	0.68 ± 0.10
E (20 mol % Chol)	1.8 ± 0.1	N (50 mol % CTL)	0.55 ± 0.14

$$S_{ab} = \frac{1}{2}\langle 3\cos\theta_a\ 3\cos\theta_b - \delta_{ab}\rangle \quad a, b = x, y, z \tag{12}$$

where in turn θ_a (or θ_b) is the angle made by ath (or bth) molecular axis with the bilayer normal and δ_{ab} is the Kronecker delta ($\langle\rangle$ denotes both ensemble and time averaging). $-S_{CD}$ can vary between 0.5 (full order along the bilayer normal) and −0.25 (full order along the bilayer plane), whereas S_{CD} = 0 denotes isotropic orientation.

Figure 9 shows the calculated $-S_{CD}$ profiles for both *sn*-1 (left panels) and *sn*-2 (right panels) POPC acyl chains for all simulated systems. The profiles for the POPC and POPC/Chol systems obtained agreed with both experimental[66,67] and simulated[59,61,68,69] reported data. In particular, as Chol amount is increased, higher order parameters are obtained.

From Figure 9A,B, it is already apparent that simple insertion of ∼1.5 mol % Chol leads to a noticeable increase in the order parameters, unlike insertion of either DHE or CTL (which essentially leave the $-S_{CD}$ profile unaltered), in agreement with the molecular area and bilayer thickness data of Table 2. Increasing the Chol mole fraction to ∼20 mol % (Figure 9C,D) and ∼50 mol % (Figure 9G,H) leads to higher $-S_{CD}$ values, due to the ordering effect of Chol. In these plots, it can be seen that replacement of 2 Chol molecules with 2 DHE or 2 CTL molecules generally leads to a decrease in the calculated $-S_{CD}$ profile, but the variation becomes insignificant in the latter case, similarly to that of molecular areas and bilayer thickness. However, replacement of all Chol molecules with DHE or CTL leads to a clear decrease of $-S_{CD}$ for 20 mol % sterol, even if the bilayers are still clearly more ordered than the ld systems of Figure 9A,B. In most of the discussed results it seems that replacement of Chol with DHE decreases $-S_{CD}$ to a larger extent than replacement with CTL (also in agreement with the data of Table 2). Curiously, for 50 mol % total sterol, it appears that DHE is as efficient at ordering the end region of both acyl chains as both CTL and (even) Chol. The reason for this effect (which does not extend to the first C atoms) is not totally clear, but is most probably related to the different side chain of DHE, which includes a rigid *trans*-double bond which is absent in the other sterols.

$-S_{CD}$ values were also calculated for varying distance R to the closest sterol molecule in the same bilayer leaflet, as illustrated in Figure 10 for the POPC/2 sterol molecules systems. It is observed that all sterols order nearby acyl chains. Curiously, CTL and DHE induce a higher degree of ordering (compared to Chol) of the nearest POPC molecules at both ends of the *sn*-1 chains in these systems. However, beyond the two immediate lipid shells (R > 1.2 nm), $-S_{CD}$ is higher for Chol system than for those with the fluorescent sterols. Because the vast majority of POPC molecules fall into this category, overall order is higher in system B (panel A) than in systems C and D (panels B and C, respectively); that is, Chol leads to an overall increased order, despite appearing to have a slightly lower ability to increase $-S_{CD}$ of the nearest acyl chains. In any case, it should be emphasized that, for these calculations, POPC chains nearest the two sterol molecules in each simulation are relatively few, implying that the corresponding profiles are affected by considerable uncertainty.

Another way to look at this effect is to calculate the tilt of the *sn*-1 acyl chain (defined as the vector connecting carbons 36 and 49, following the atom numbering displayed in Figure 1) relative to the bilayer normal for different ranges of R values, as shown in Figure 11. The same trends are apparent, with the Chol systems having the lowest global average acyl chain tilts (31.7° ± 0.3° on average, compared to 32.3° ± 0.4° for DHE and 32.0° ± 0.5° for CTL), despite displaying larger tilt of the nearest acyl chains (27° ± 3° on average, compared to 23° ± 3° for DHE and 23° ± 2 for CTL). However, these differences are again not significant, and the main conclusion is that all three sterols are able to order neighboring POPC chains.

We also looked at the potential effect of the probes upon the orientation of Chol in the ternary systems with 20 mol % and 50 mol % total sterol. Figure 12 shows the angular distributions of the angle between the Chol long axis and the bilayer normal in these trajectories, compared to that obtained for the corresponding binary POPC/Chol systems. It is apparent that probe effects are minor, with a small shift to higher tilts noticeable for DHE in the 20 mol % sterol systems, and no appreciable alterations for 50 mol % sterol. This increased tilt of Chol in the presence of DHE for 20 mol % sterol is probably induced by the higher tilting of DHE itself. For the 50 mol % sterol systems, as the relative

dx.doi.org/10.1021/jp312026u | J. Phys. Chem. B 2013, 117, 5806−5819

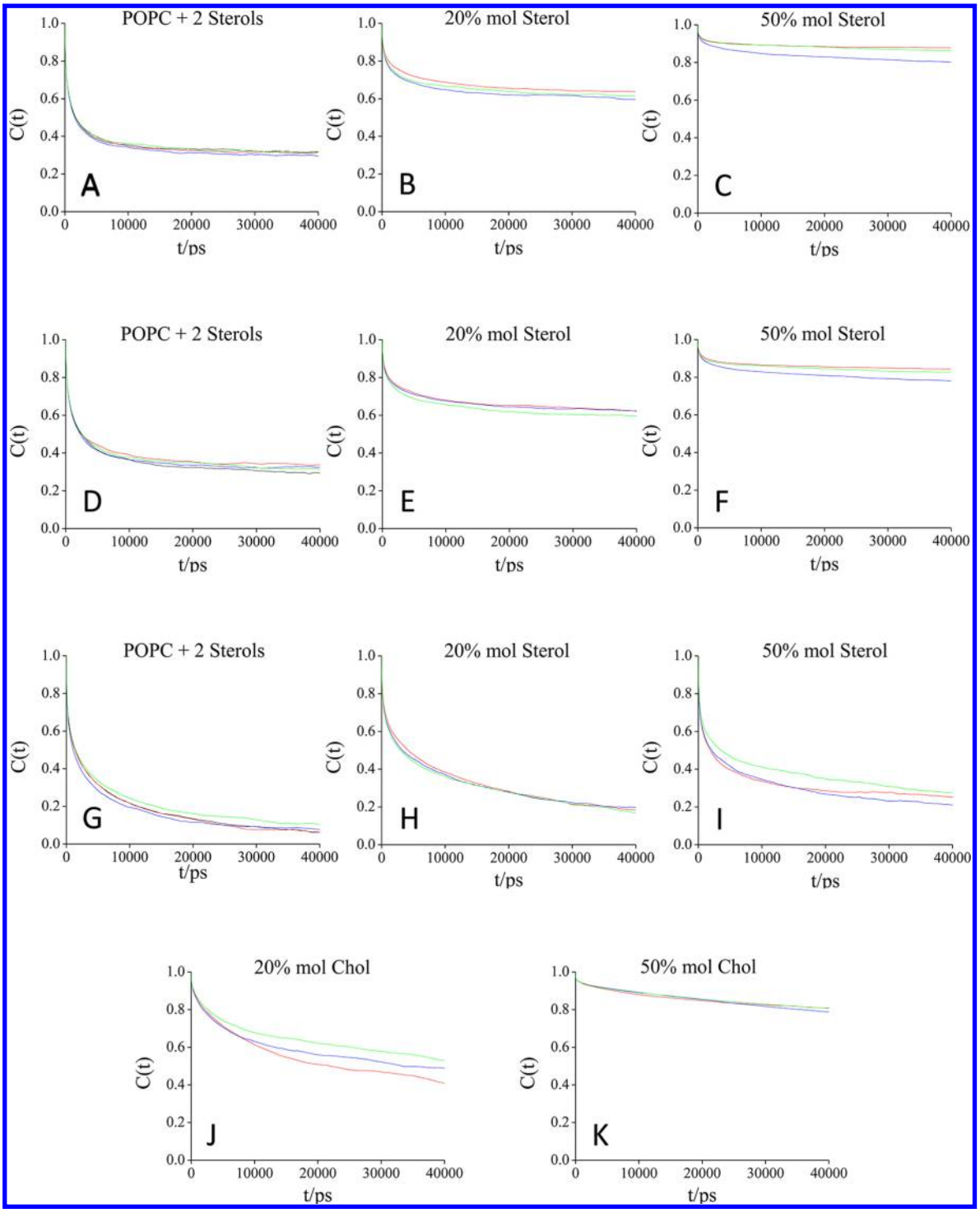

Figure 13. Rotational autocorrelation functions $C(t)$ for the POPC *sn*-1 acyl chain (A–C), POPC *sn*-2 acyl chain (D–F), POPC P–N (G–I), and Chol long axis (J,K) in binary POPC/sterol mixtures with ~1.5 mol % (A,D,G), 20 mol % (B,E,H) or 50 mol % (C,F,I) sterol, or ternary POPC/Chol/sterol mixtures, with 2 sterol molecules and 20 mol % (J) or 50 mol % (K) total sterol. In all plots, black, red, blue, and green lines refer to POPC, Chol, DHE, and CTL, respectively.

amount of fluorescent sterol is diminished, and the tilt of DHE is closer to that of Chol, this effect is no longer noticeable.

Probe Effects on Host Lipid Dynamics. For the purpose of assessing possible differential effects of the sterols on POPC translational dynamics, two-dimensional mean square displacements of POPC were calculated and are shown in Figure S3 in the Supporting Information file for the systems where Chol was completely replaced by either DHE or CTL (for the 20 mol % and 50 mol % Chol systems where only two sterol molecules were replaced, variations upon replacement were minor; data not shown). The corresponding lateral diffusion coefficients of POPC obtained using eqs 1 and 2 are shown in Table 3.

It is clear that the sterol-induced ordering and condensation discussed above is reflected in lower D_{lat} values as the total sterol concentration increases. On the other hand, replacement of Chol with one of the fluorescent sterols leads to higher D_{lat}, which

dx.doi.org/10.1021/jp312026u | J. Phys. Chem. B 2013, 117, 5806–5819

correlates with the higher molecular areas (Table 2) and lower order parameters (Figure 9). Because DHE and CTL are less efficient than Chol at condensing and ordering the bilayer, POPC molecules show slightly faster translational dynamics in the presence of the fluorescent sterols than in the presence of Chol. Generally, these effects are larger for DHE than for CTL (with the exception of the 20 mol % composition, for which they are essentially identical), also in agreement with the data shown previously.

Rotational autocorrelation functions $C(t)$ were calculated for several host lipid POPC axes (POPC *sn*-1 (C36−C49 vector), *sn*-2 (C17−C51 vector), and P−N), as well as for Chol long axis (C2−C20 vector), and are shown in Figure 13. As expected, upon loading with Chol, $C(t)$ of POPC acyl chains and Chol long axis decay more slowly, whereas that of the more external P−N axis is almost unaltered. For the latter vector, and irrespective of total sterol content, replacement of Chol with either DHE or CTL led only to very small changes in $C(t)$ (Figure 13G−I). This was expected, as all three bilayer-inserted sterols are located deeper than the phospholipid headgroup. Regarding both POPC acyl chains (Figure 13A−F), complete replacement of Chol with one of the fluorescent probes also resulted in modest effects, although rotational tumbling is slightly faster in the systems containing DHE (blue lines) for 50 mol % sterol (Figure 13C,F), due to the lower membrane-ordering efficiency of this sterol, more evident for high sterol content. Finally, rotation of Chol long axis is apparently slightly slower in the presence of the two fluorescent sterol molecules for 20 mol % total sterol (Figure 13J). For 50 mol % sterol, no noticeable differences are observed, again probably due to the low relative degree of substitution (Figure 13K).

CONCLUDING REMARKS

This work aimed at a comparison of the atomic-scale behavior of intrinsically fluorescent sterols DHE and CTL with that of Chol, the molecule they are used to emulating in experimental studies. Two main general conclusions may be inferred. First, in general terms, both DHE and CTL are adequate analogues of Chol. Both fluorescent sterols have similar transverse locations to that of Chol, position themselves upright in the bilayer, and induce ordering of POPC bilayers, albeit to extents slightly lower than that of Chol, in accordance with experimental findings.[14,18] No secondary maxima were found in the sterol long axis distribution even for disordered bilayers, at variance with side chain-labeled BODIPY-Chol.[16] Probe rotational and translational dynamics were also similar to (generally slightly faster than) those of Chol. Second, of the two studied fluorescent sterols, CTL is the one with behavior closest to that of Chol. This pattern, which could be anticipated from molecular structures, can be found in sterol long axis tilts (larger for DHE), area/POPC (higher for DHE), membrane thickness, POPC acyl chain order parameters (both lower for DHE), host lipid dynamics (faster for DHE), and RDFs of Chol around each sterol. In particular, the previously proposed inverse correlation between sterol tilt and ability to order the bilayers[26] was verified.

Our observations may be related to a recent MD study involving Chol, 7-DHC, and demosterol.[28] Both of these sterols differ from Chol by having an additional double bond, which in 7-DHC is located in the steroid ring (7-DHC has in intermediate structure between those of Chol and CTL), whereas in desmosterol it lies in the aliphatic chain. The authors of this study conclude that whereas all sterols display similar behavior in bilayers of DOPC (which has two unsaturated acyl chains), their ordering efficiencies vary considerably in fluid bilayers of saturated acyl-chain lipid DPPC, in the order Chol >7-DHC > desmosterol. Therefore, the effect of introducing an additional double bond in the sterol side-chain appears to be more significant than adding a double bond in the steroid ring, conjugated to that already existing in Chol. In our work, noticeable differences in sterol behavior were observed in bilayers of POPC, composed of one saturated and one unsaturated acyl chain. Whereas CTL closely emulates the behavior of Chol (with which it shares an identical side-chain, differing only in having three conjugated double bonds—instead of one for Chol—in the steroid ring), DHE has a smaller ordering efficiency, which may be related to its modifications (additional double bond and methyl group) in the side-chain.

We can therefore conclude that CTL is a slightly superior mimic of Chol's behavior in membranes. However, actual use of either sterol must also take into account the more limited availability of CTL compared to the naturally occurring DHE. Finally, it should be noted that, whereas these sterols are adequate structural and dynamical analogues of Chol, their spectroscopic properties (maximal emission in the UV region, relatively low molar absorption, photostability, and emission quantum yield) are not optimal, as commented elsewhere.[12] This could tempt experimental researchers to use side chain or even cholesteryl ester probes as fluorescent replacements for Chol. However, both UV wide-field imaging and multiphotonic microscopy of CTL or DHE offer great potential to circumvent these limitations,[70] with the advantages of proper emulation of Chol's behavior, as demonstrated in the present work.

ASSOCIATED CONTENT

Supporting Information

Final snapshots for all simulations; time variation of molecular area for all lipid and probe species in all systems; mean square displacements of POPC. This material is available free of charge via the Internet at http://pubs.acs.org.

AUTHOR INFORMATION

Corresponding Author

*Telephone: +351 239488485. Fax: +351 239827126. E-mail: lloura@ff.uc.pt.

Notes

The authors declare no competing financial interest.

ACKNOWLEDGMENTS

The authors acknowledge funding by FEDER, through the COMPETE program, and by FCT (Fundação para a Ciência e a Tecnologia, Portugal), project reference FCOMP-01-0124-FEDER-010787 (FCT PTDC/QUI-QUI/098198/2008). J.R.R. acknowledges FCT and the same Project for a research grant.

REFERENCES

(1) Ipsen, J. H.; Karlström, G.; Mouritsen, O. G.; Wennerström, H.; Zuckermann, M. J. Phase Equilibria in the Phosphatidylcholine-Cholesterol System. *Biochim. Biophys. Acta* **1987**, *905*, 162−172.

(2) Vist, M. R.; Davis, J. H. Phase Equilibria of Cholesterol/Dipalmitoylphosphatidylcholine Mixtures: 2H Nuclear Magnetic Resonance and Differential Scanning Calorimetry. *Biochemistry* **1990**, *29*, 451−464.

(3) Almeida, P. F.; Vaz, W. L.; Thompson, T. E. Lateral Diffusion in the Liquid Phases of Dimyristoylphosphatidylcholine/Cholesterol Lipid Bilayers: a Free Volume Analysis. *Biochemistry* **1992**, *31*, 6739−6747.

(4) Thewalt, J. L.; Bloom, M. Phosphatidylcholine: Cholesterol Phase Diagrams. *Biophys. J.* **1992**, *63*, 1176−1181.
(5) Gennis, R. B. *Biomembranes: Molecular Structure and Function*; Springer: New York, 1989.
(6) Ipsen, J. H.; Mouritsen, O. G.; Bloom, M. Relationships Between Lipid Membrane Area, Hydrophobic Thickness and Acyl Chain Orientational Order. The Effects of Cholesterol. *Biophys. J.* **1990**, *57*, 405−412.
(7) Needham, D.; Nunn, R. S. Elastic Deformation and Failure of Lipid Bilayer Membranes Containing Cholesterol. *Biophys. J.* **1990**, *58*, 997−1009.
(8) Yeagle, P. L. Modulation of Membrane Function by Cholesterol. *Biochimie* **1991**, *73*, 1303−1310.
(9) Simons, K.; Vaz, W. L. C. Model Systems, Lipid Rafts, and Cell Membranes. *Annu. Rev. Biophys. Biomol. Struct.* **2004**, *33*, 269−295.
(10) Lingwood, D.; Simons, K. Lipid Rafts as a Membrane Organizing Principle. *Science* **2010**, *327*, 46−50.
(11) de Almeida, R. F. M.; Loura, L. M. S.; Prieto, M. Membrane Lipid Domains and Rafts: Current Applications of Fluorescence Lifetime Spectroscopy and Imaging. *Chem. Phys. Lipids* **2009**, *157*, 61−77.
(12) Wüstner, D. Fluorescent Sterols as Tools in Membrane Biophysics and Cell Biology. *Chem. Phys. Lipids* **2007**, *146*, 1−25.
(13) Loura, L. M. S.; Fedorov, A.; Prieto, M. Exclusion of a Cholesterol Analog from the Cholesterol Rich Phase in Model Membranes. *Biochim. Biophys. Acta* **2001**, *1511*, 236−243.
(14) Scheidt, H. A.; Müller, P.; Herrmann, A.; Huster, D. The Potential of Fluorescent and Spin Labelled Steroid Analogs to Mimic Natural Cholesterol. *J. Biol. Chem.* **2003**, *278*, 45563−45569.
(15) Shaw, J. E.; Epand, R. F.; Epand, R. M.; Li, Z.; Bittman, R.; Yip, C. M. Correlated Fluorescence Atomic Force Microscopy of Membrane Domains: Structure of Fluorescence Probes Determines Lipid Localization. *Biophys. J.* **2006**, *90*, 2170−2178.
(16) Hölttä-Vuori, M.; Uronen, R. L.; Repakova, J.; Salonen, E.; Vattulainen, I.; Panula, P.; Li, Z.; Bittman, R.; Ikonen, E. BODIPY Cholesterol. A New Tool to Visualize Sterol Trafficking in Living Cells and Organisms. *Traffic (Copenhagen, Den.)* **2008**, *9*, 1839−1849.
(17) Garvik, O.; Benediktson, P.; Simonsen, A. C.; Ipsen, J. H.; Wüstner, D. The Fluorescent Cholesterol Analog Dehydroergosterol Induces Liquid Ordered Domains in Model Membranes. *Chem. Phys. Lipids* **2009**, *159*, 114−118.
(18) Staneva, G.; Chachaty, C.; Wolf, C.; Quinn, P. J. Comparison of the Liquid Ordered Biayer Phases Containing Cholesterol or 7-Dehydroergosterol in Modelling Smith Lemli Opitz Syndrome. *J. Lipid Res.* **2010**, *51*, 1810−1822.
(19) Mouritsen, O. G.; Zuckermann, M. J. What's so Special about Cholesterol? *Lipids* **2004**, *39*, 1101−1113.
(20) Lyubartsev, A. P.; Rabinovich, A. L. Recent Development in Computer Simulations of Lipid Bilayers. *Soft Matter* **2011**, *7*, 25−39.
(21) Loura, L. M. S.; Ramalho, J. P. P. Fluorescent Membrane Probes' Behaviour in Lipid Bilayers: Insights from Molecular Dynamics Simulations. *Biophys. Rev.* **2009**, *1*, 141−148.
(22) Loura, L. M. S.; Ramalho, J. P. P. Recent Developments in Molecular Dynamics Simulations of Fluorescent Membrane Probes. *Molecules* **2011**, *16*, 5437−5452.
(23) Smondyrev, A. M.; Berkowitz, M. L. Molecular Dynamics Simulation of the Structure of Dimyristoylphosphatidylcholine Bilayers with Cholesterol, Ergosterol and Lanosterol. *Biophys. J.* **2001**, *80*, 1649−1658.
(24) Róg, T.; Pasenkiewicz-Gierula, M.; Vattulainen, I.; Karttunen, M. What Happens if Cholesterol Is Made Smoother: Importance of Methyl Substituents in Cholesterol Ring Structure on Phosphatidylcholine−Sterol Interaction. *Biophys. J.* **2007**, *92*, 3346−3357.
(25) Ollila, O. H. S.; Róg, T.; Karttunen, M.; Vattulainen, I. Role of Sterol Type on Lateral Pressure Profiles of Lipid Membranes Affecting Membrane Protein Functionality: Comparison Between Cholesterol, Desmosterol, 7-Dehydrocholesterol and Ketosterol. *J. Struct. Biol.* **2007**, *159*, 311−323.
(26) Vainio, S.; Jansen, M.; Koivusalo, M.; Róg, T.; Karttunen, M.; Vattulainen, I.; Ikonen, E. Significance of Sterol Structural Specificity. Desmosterol cannot replace Cholesterol in Lipid Rafts. *J. Biol. Chem.* **2006**, *281*, 348−355.
(27) Aittoniemi, J.; Róg, T.; Niemela, P.; Pasenkiewicz-Gierula, M.; Karttunen, M.; Vattulainen, I. Tilt: Major Factor in Sterols' Ordering Capability in Membranes. *J. Phys. Chem. B* **2006**, *110*, 25562−25564.
(28) Róg, T.; Vattulainen, I.; Jansen, M.; Ikonen, E.; Karttunen, M. Comparison of Cholesterol and Its Direct Precursors Along The Biosynthetic Pathway: Effects of Cholesterol, Desmosterol and 7-Dehydrocholesterol on Saturated and Unsaturated Lipid Bilayers. *J. Chem. Phys.* **2008**, *129*, 154508.
(29) Berger, O.; Edholm, O.; Jähnig, F. Molecular Dynamics Simulations of a Fluid Bilayer of Dipalmitoylphosphatidylcholine at Full Hydration, Constant Pressure and Constant Temperature. *Biophys. J.* **1997**, *72*, 2002−2013.
(30) Hoff, B.; Strandberg, E.; Ulrich, A. S.; Tieleman, D. P.; Posten, C. ^{2}H-NMR Study and Molecular Dynamics Simulation of the Location, Alignment and Mobility of Pyrene in POPC Bilayers. *Biophys. J.* **2005**, *88*, 1818−1827.
(31) Berendsen, H. ; Postma, J.; van Gunsteren, W. ; Hermans, J. *Intermolecular Forces*; Reidel: Dordrecht, The Netherlands, 1981.
(32) Höltje, M.; Förster, T.; Brandt, B.; Engels, T.; von Rybinski, W.; Höltje, H. Molecular Dynamics Simulations of Stratum Corneum Lipid Models: Fatty Acids and Cholesterol. *Biochim. Biophys. Acta* **2001**, *1511*, 156−167.
(33) Becke, A. Density-Functional Thermochemistry III. The Role of Exact Exchange. *J. Chem. Phys.* **1993**, *98*, 5648−5652.
(34) Lee, C.; Yang, W.; Parr, R. Development of the Colle-Salvetti Correlation-Energy Formula into a Functional of the Electron Density. *Phys. Rev. [Sect.] B* **1988**, *37*, 785−789.
(35) Vosko, S.; Wilk, L.; Nussair, M. Accurate Spin-Dependant Electron Liquid Correlation Energies for Local Spin Density Calculations: a Critical Analysis. *Can. J. Phys.* **1980**, *58*, 1200−1211.
(36) Stephens, P.; Devlin, F.; Chabalowski, C.; Frisch, M. Ab Initio Calculation of Vibrational Absorption and Circular Dichroism Spectra Using Density Functional Force Fields. *J. Phys. Chem.* **1994**, *98*, 11623−11627.
(37) Granovsky, A. Firefly v 7.1.G, http://classic.chem.msu.su/gran/firefly/index.html.
(38) Schüttelkopf, A.; Aalten, D. PRODRG: a Tool for High-Throughput Crystallography of Protein-Ligand Complexes. *Acta Crystallogr.* **2004**, *60*, 1355−1363.
(39) Humphrey, W.; Dalke, A.; Schulten, K. VMD − Visual Molecular Dynamics. *J. Molec. Graphics* **1996**, *14*, 33−38.
(40) Murzyn, K.; Róg, T.; Jezierski, G.; Takaoka, Y.; Pasenkiewicz-Gierula, M. Effects of Phospholipid Unsaturation on the Membrane/Water Interface: a Molecular Simulation Study. *Biophys. J.* **2001**, *81*, 170−183.
(41) Berendsen, H.; Postma, J.; DiNola, A.; Haak, J. Molecular Dynamics with Coupling to an External Bath. *J. Chem. Phys.* **1984**, *81*, 3684−3690.
(42) Myamoto, S.; Kollman, P. SETTLE an Analytical Version of the SHAKE and RATTLE Algorithms for Rigid Water Models. *J. Comput. Chem.* **1992**, *13*, 952−962.
(43) Hess, B.; Bekker, H.; Berendsen, H.; Fraaije, J. LINCS: a Linear Constraint Solver for Molecular Simulations. *J. Comput. Chem.* **1997**, *18*, 1463−1472.
(44) Feenstra, K.; Hess, B.; Berendsen, H. Improving efficiency of Large Timescale Molecular Dynamics Simulations of Hydrogen-Rich Systems. *J. Comput. Chem.* **1999**, *20*, 786−798.
(45) Anézo, C.; de Vries, A. H.; Höltje, H. D.; Tieleman, D. P.; Marrink, S. J. Methodological Issues in Lipid Bilayer Simulations. *J. Phys. Chem. B* **2003**, *107*, 9424−9433.
(46) Essman, U.; Perela, L.; Berkowitz, M.; Darden, T.; Lee, H.; Pedersen, L. A Smooth Particle Mesh Ewald Method. *J. Chem. Phys.* **1995**, *103*, 8577−8592.
(47) Berendsen, H.; van der Spoel, D.; van Drunen, R. GROMACS: a Message-Passing Parallel Molecular Dynamics Implementation. *Comput. Phys. Commun.* **1995**, *91*, 43−56.

(48) Lindhal, E.; Hess, B.; van der Spoel, D. GROMACS 3.0: a Package for Molecular Simulation and Trajectory Analysis. *J. Mol. Modeling* **2001**, *7*, 306−317.
(49) van der Spoel, D.; Lindhal, E.; Hess, B.; Groenhof, G.; Mark, A.; Berendsen, H. GROMACS: Fast, Flexible and Free. *J. Comput. Chem.* **2005**, *26*, 1701−1718.
(50) Hess, B.; Kutzner, C.; van der Spoel, D.; Lindhal, E. GROMACS 4: Algorithms for Highly Efficient, Load-Balanced, and Scalable Molecular Simulation. *J. Chem. Theory Comput.* **2008**, *4*, 435−447.
(51) Róg, T.; Pasenkiewicz-Gierula, M. Cholesterol Effects on a Mixed-Chain Phosphatidylcholine Bilayer: a Molecular Dynamics Simulation Study. *Biochimie* **2006**, *88*, 449−460.
(52) Kinosita, K.; Kawato, S.; Ikegami, A. A Theory of Fluorescence Polarization Decay in Membranes. *Biophys. J.* **1977**, *20*, 289−305.
(53) Hofsäβ, C.; Lindhal, E.; Edholm, O. Molecular Dynamics Simulatons of Phospholipid Bilayers with Cholesterol. *Biophys. J.* **2003**, *84*, 2192−2206.
(54) Voss, N.; Gerstein, M. 3V: Cavity, Channel and Cleft Volume Calculator and Extractor. *Nucleic Acid Res.* **2010**, *38*, 555−562.
(55) Greenwood, A. I.; Tristram-Nagle, S.; Nagle, J. F. Partial Molecular Volumes of Lipids and Cholesterol. *Chem. Phys. Lipids.* **2006**, *143*, 1−10.
(56) Lantzsch, G.; Binder, H.; Heerklotz, H.; Wendling, M.; Klose, G. Surface Areas and Packing Constraints in POPC/$C_{12}EO_n$ Membranes. *Biophys. Chem.* **1996**, *58*, 289−302.
(57) Konig, B.; Dietrich, U.; Klose, G. Hydration and Structural Properties of Mixed Lipid/Surfactant Model Membranes. *Langmuir* **1997**, *13*, 525−532.
(58) Smaby, J.; Momsen, M.; Brockman, H.; Brown, R. Phosphatidylcholine Acyl Unsaturation Modulates the Decrease in Interfacial Elasticity Induced by Cholesterol. *Biophys. J.* **1997**, *73*, 1492−1505.
(59) Bockmann, R.; Hac, A.; Heimburg, T.; Grubmuller, H. Effects of Sodium Chloride on a Lipid Bilayer. *Biophys. J.* **2003**, *85*, 1647−1655.
(60) Mukhopadhyay, P.; Vogel, H.; Tieleman, D. Distribution of Pentachlorophenol in Phospholipid Bilayers: a Molecular Dynamics Study. *Biophys. J.* **2004**, *86*, 337−345.
(61) Gurtovenko, A.; Anwar, J. Interaction of Ethanol with Biological Membranes: the Formation of Non-Bilayer Structures within the Membrane Interior and their Significance. *J. Phys. Chem. B* **2009**, *113*, 1983−1992.
(62) Pandit, S.; Chiu, S.; Jakobsson, E.; Grama, A.; Scott, H. Cholesterol Packing around Lipids with Saturated and Unsaturated Chains: a Simulation Study. *Langmuir* **2008**, *24*, 6858−6865.
(63) Hung, W.; Lee, M.; Chen, F.; Huang, H. The Condensing Effect of Cholesterol in Lipid Bilayers. *Biophys. J.* **2007**, *92*, 3960−3967.
(64) Róg, T.; Pasenkiewicz-Gierula, M.; Vattulainen, I.; Karttunen, M. Ordering Effects of Cholesterol and its Analogues. *Biochim. Biophys. Acta* **2009**, *1788*, 97−121.
(65) Douliez, J.; Leonard, A.; Dufourc, E. Restatement of Order Parameters in Biomembranes: Calculation of C-C Bond Order Parameters from C-D Quadrupolar Splittings. *Biophys. J.* **1995**, *68*, 1727−1739.
(66) Seelig, J.; Waespesarcevic, N. Molecular Order in cis and trans Unsaturated Phospholipid Bilayers. *Biochemistry* **1978**, *17*, 3310−3315.
(67) Klose, G.; Madler, B.; Schafer, H.; Schneider, K. Structural Characterization of POPC and $C_{12}E_4$ in their Mixed Membranes at Reduced Hydration by Solid State ^2H NMR. *J. Phys. Chem. B* **1999**, *103*, 3022−3029.
(68) Patra, M.; Salonen, E.; Terama, E.; Vattulainen, I.; Faller, R.; Lee, B.; Holopainen, J.; Karttunen, M. Under the Influence of Alcohol: the Effect of Ethanol and Methanol on Lipid Bilayers. *Biophys. J.* **2006**, *90*, 1121−1135.
(69) Falck, E.; Patra, M.; Karttunen, M.; Hyvönen, M.; Vattulainen, I. Lessons of Slicing Membranes: Interplay of Packing, Free Area, and Lateral Diffusion in Phospholipid/Cholesterol Bilayers. *Biophys. J.* **2004**, *87*, 1076−1091.
(70) Wüstner, D.; Brewer, J. R.; Bagatolli, L.; Sage, D. Potential of Ultraviolet Wide-Field Imaging and Multiphoton Microscopy for Analysis of Dehydroergosterol in Cellular Membranes. *Microsc. Res. Tech.* **2011**, *74*, 92−108.